

Exploring Hydraulic Behavior of Barrage Using HEC-RAS at Semangir River Jember Regency

Sefti Aryani, Entin Hidayah*, Gusfan Halik

Department of Civil Engineering, Universitas Jember, Jember, INDONESIA

*Corresponding author: entin.teknik@unej.ac.id

SUBMITTED 01 September 2024 REVISED 06 January 2025 ACCEPTED 03 February 2025

ABSTRACT Flooding significantly impacts communities living along riverbanks, causing severe damage to infrastructure and properties. The flood event on January 9, 2022, in Bumi Mangli Permai and Mangli Residence Housing heavily damaged access roads. Effective flood control is essential to mitigate these risks, and one viable solution is the implementation of long storage systems, particularly barrage. This study explores the hydraulic behavior of the Semangir River in Jember Regency using the HEC-RAS program to model both fixed weir and barrage. Utilizing the SUH Nakayasu method, variability of peak discharges for 25-year, 50-year, and 100-year return periods were estimated. The analysis revealed that the existing fixed weir is inadequate for the 50-year return period. The tool used in hydraulic analysis is HEC-RAS. The characteristics tested include velocity, Froude number, water surface elevation, and energy gradient. However, the result of simulations indicates that a barrage with gate dimensions of 1.5 m 1.75 m offers improved hydraulic conditions, reducing water surface elevation and flow velocity compared to both the existing and initially design weirs. These findings support the adoption of barrage as an effective flood control strategy for the Semangir River. The study demonstrates that barrages are more effective than fixed weirs in managing hydraulic characteristics during floods, particularly variability of peak discharges 25- and 50-year return periods. Barrages with larger gates reduce downstream flow velocity, turbulence, and energy grade elevation, minimizing structural risks and overflow. Their adaptive capability highlights the importance of gate size and design for optimizing hydraulic performance and flood management efficiency.

KEYWORDS Flood control, HEC-RAS, Hydraulic behavior, Long storage, Barrage, Return periods

© The Author(s) 2025. This article is distributed under a Creative Commons Attribution-ShareAlike 4.0 International license.

1 INTRODUCTION

Flooding is one of the natural phenomena that occurs due to high rainfall intensity, resulting in excess water that is not accommodated by the system (Balaian et al., 2024). The area around the river becomes a vulnerable area affected by flooding during the rainy season. Floods generally cause damage to infrastructure such as roads, bridges, and water structures, making them a primary cause of infrastructure damage worldwide (Ogras and Onen, 2020). On January 9, 2022, severe flooding affected Bumi Mangli Permai and Mangli Residence Housing, causing significant damage to facilities and infrastructure, including the downstream section of the Semangir Weir (BNPB, 2022).

High flood discharge is directly proportional to water level. As the water level rises, the velocity of the water flow increases after passing through the spillway structure, which can lead to erosion (scouring) and sedimentation (deposition) in river channels (Salmasi and Abraham, 2023; Syaifudin, 2022). Additionally, high flow velocity can cause cavitation, which is the formation of air bubbles in the water that can disrupt the stability of the spillway structure (Paksi et al., 2021). Effective flood control measures are needed to minimize property and life losses, with one potential solution being the use of long storage as a flood mitigation strategy.

The use of long-term storage can enhance water capacity in the riverbed and reduce flood peaks through the operation of a barrage (Dickel and Theobald, 2024; Kus-tamar et al., 2019; Zaffar et al., 2023). Installing barrages on the Semangir River can function as long-term water storage, helping to maintain water discharge during the dry season, while the gates can be opened to control flooding during the rainy season. Increasing the gate opening size affects the upstream and downstream water levels, with larger gate openings resulting in lower upstream water levels and higher downstream water levels. The use of barrages can be considered, as barrages control the amount of river discharge (outflow) during floods to reduce downstream damage barrage management can contribute to flood reduction on the Inn River (Dickel and Theobald, 2024; Eizeldin et al., 2023).

Previous studies in flood control and hydraulic modeling research have demonstrated significant advancements in the use of software such as HEC-RAS for simulating water flow and analyzing flood impacts. HEC-RAS, developed by the US Army Corps of Engineers, is widely used for river flow modeling and floodplain analysis. Both 1D and 2D modeling with HEC-RAS have proven effective in analyzing flow conditions and

predicting flood inundation (Ghimire et al., 2020; Mitsopoulos et al., 2022). HEC-RAS enables highly accurate river flow simulations, with results that closely match historical data and field measurements (Hidayah et al., 2022; Prawira et al., 2024). HEC-RAS supports both one-dimensional (1D) and two-dimensional (2D) simulations, enabling more detailed analysis based on design rainfall input data (Guido et al., 2023; Sari et al., 2018). Additionally, HEC-RAS is capable of simulating lateral structures, operating gates, weirs, and other constructions along the riverbanks, making it effective for flood risk adaptation (Sarchani et al., 2020).

This study addresses existing gaps by applying the HEC-RAS model to explore and compare the effectiveness of weirs and barrages in flood control on the Semangir River. The research evaluates differences between 1D flow modeling in the context of flood control, as well as the specific impacts of cavitation and high flow velocity on spillway structures and infrastructure. By utilizing the case studies of Bumi Mangli Permai and Mangli Residence Housing, this research provides new insights into the application of HEC-RAS to enhance the understanding of flood mitigation and the effectiveness of flood control designs in practice.

2 METHODOLOGY

2.1 Study Area

This research was conducted in the Semangir tributary located in the Bedadung watershed, Jember Regency, with a sub-watershed area of 17.31 km², as shown in Figure 1. The Semangir Weir is in Kaliwates District at coordinates 8°10'59.01" South Latitude and 113°39'9.77" East Longitude.

2.2 Data Collection

The data used in this study are shown in Table 1, which provides information on the type, source, and use of the data.

2.3 Research Stages

The methodology used in the evaluation and simulation of the Semangir Weir consists of three stages, as shown in Figure 2. The first stage involves processing rainfall data and watershed characteristics. Stage 2 entails conducting a hydrological analysis to determine the flood design. The final stage involves creating a hydraulic model with the scenario: the fixed weir and barrage using HEC-RAS.

2.4 Hydrological Analysis

The hydrological analysis uses topographic and rainfall data. Hydrological calculations begin with data filtering. The data used is annual maximum rainfall. Data consistency tests are then conducted using the RAPS method. The Thiessen polygon method is used to obtain the influence ratio of each station, and then, based on the influence ratio of each station and rainfall data, regional rainfall data is obtained.

Frequency analysis and design of rainfall use appropriate distributions based on distribution fit tests using the Chi-Square and Smirnov-Kolmogorov methods. Hourly rainfall distribution is arranged with the Alternating Block Method (ABM); this study employs the Mononobe method to calculate rainfall intensity, translating daily rainfall into shorter durations for IDF curve development. The Alternating Block Method (ABM) distributes rainfall intensities, placing peak intensity mid-duration for realistic temporal representation and the rainfall intensity calculations use the Mononobe method. Design flood discharge calculations use the Synthetic Unit Hydrograph (SUH) Nakayasu method, that's input for hydraulic analysis. Design flood discharge is verified with discharge one month before and after the flood event to obtain an appropriate return period for flood discharge.

Runoff coefficient is defined as the ratio of runoff to rainfall over a certain period, whether annual, monthly, or daily, by comparing it to river flow data. The calculation of runoff coefficient value with various land uses is done using the composite value calculation concept as in Equation (1).

$$C = \frac{\sum_{i=1}^n c_i A_i}{\sum_{i=1}^n A_i} \quad (1)$$

where C is the composite runoff coefficient, A is the ratio of land use area (km²).

Design flood discharge calculations are used to determine the design discharge that will be used according to SNI 2415:2016. The determination of each method in design discharge calculations generally depends on data availability, including rainfall data, watershed characteristics, and discharge data. The selection of methods is based on data availability and watershed characteristics, which is the Synthetic Unit Hydrograph method.

Unit hydrographs work well for small to medium-sized areas where flow characteristics can be predicted using simpler methods. For larger watersheds with more complex hydrology, flow routing methods are better because they can handle wider variations in water flow. Using unit hydrographs in smaller areas, such as sub-watersheds or smaller river catchments, is appropri-

ate because they provide accurate estimates of flow response to rainfall when the area’s hydrology is relatively uniform.

Literature shows that unit hydrographs are effective for small-scale flow analysis as they simplify the complexities of flow response to rainfall under consistent conditions. They are typically used in smaller areas with uniform flow characteristics and sufficient historical data for model development and calibration. This makes them useful for planning and designing drainage

systems and managing flood risks (Nash, 1957; Snyder, 1938).

The data needed for flood routing is insufficient. At the Semangir gauge station, flow discharge and flood history data are available for only 2 years, while at least 10 years of data are required for effective flood routing. The unit hydrograph is an appropriate choice because all the required data is available, including watershed characteristics, land use, and rainfall data.

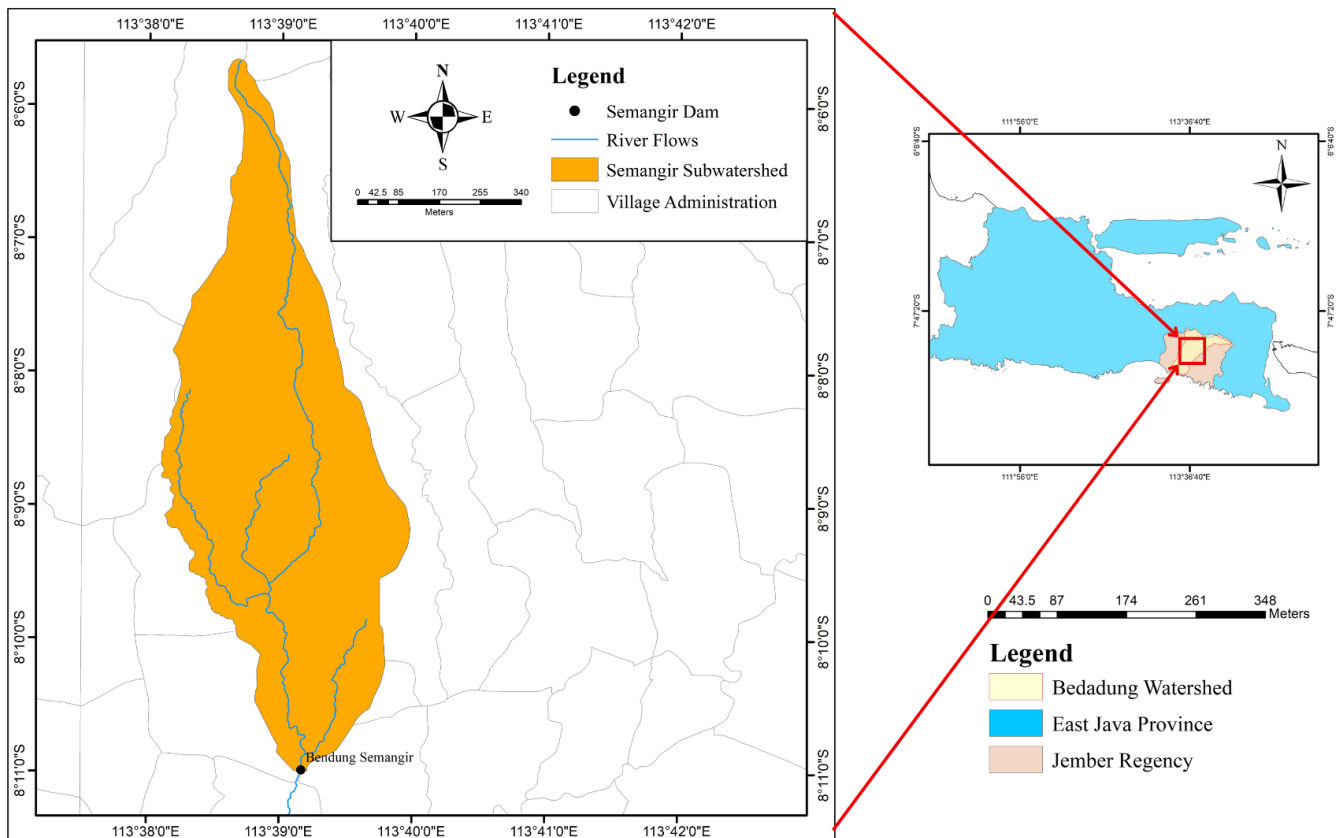


Figure 1 Study area

Table 1. Data used

Type of Data	Source of Data	Purpose
Cross-section and long-section data of Semangir River	UPT. PSDA Jember Regency	Geometric data input into HEC-RAS
Existing weir and barrage design drawings of Semangir	UPT. PSDA Jember Regency, Rambipuji Observer	Inline structure data input into HEC-RAS
Daily rainfall data from 2011-2022	UPT. PSDA Jember Regency (Semangir, Manggis, Pono, and Sembah Station)	Hydrological calculations
Semangir Weir water level data from 2021-2022	UPT. PSDA Jember Regency, Rambipuji Observer	Calibration of the existing HEC-RAS model, discharge verification
Land use map	UPT. PSDA Jember Regency	Determining runoff coefficient
Manning’s roughness coefficient of the riverbank	Survey	Modeling parameters

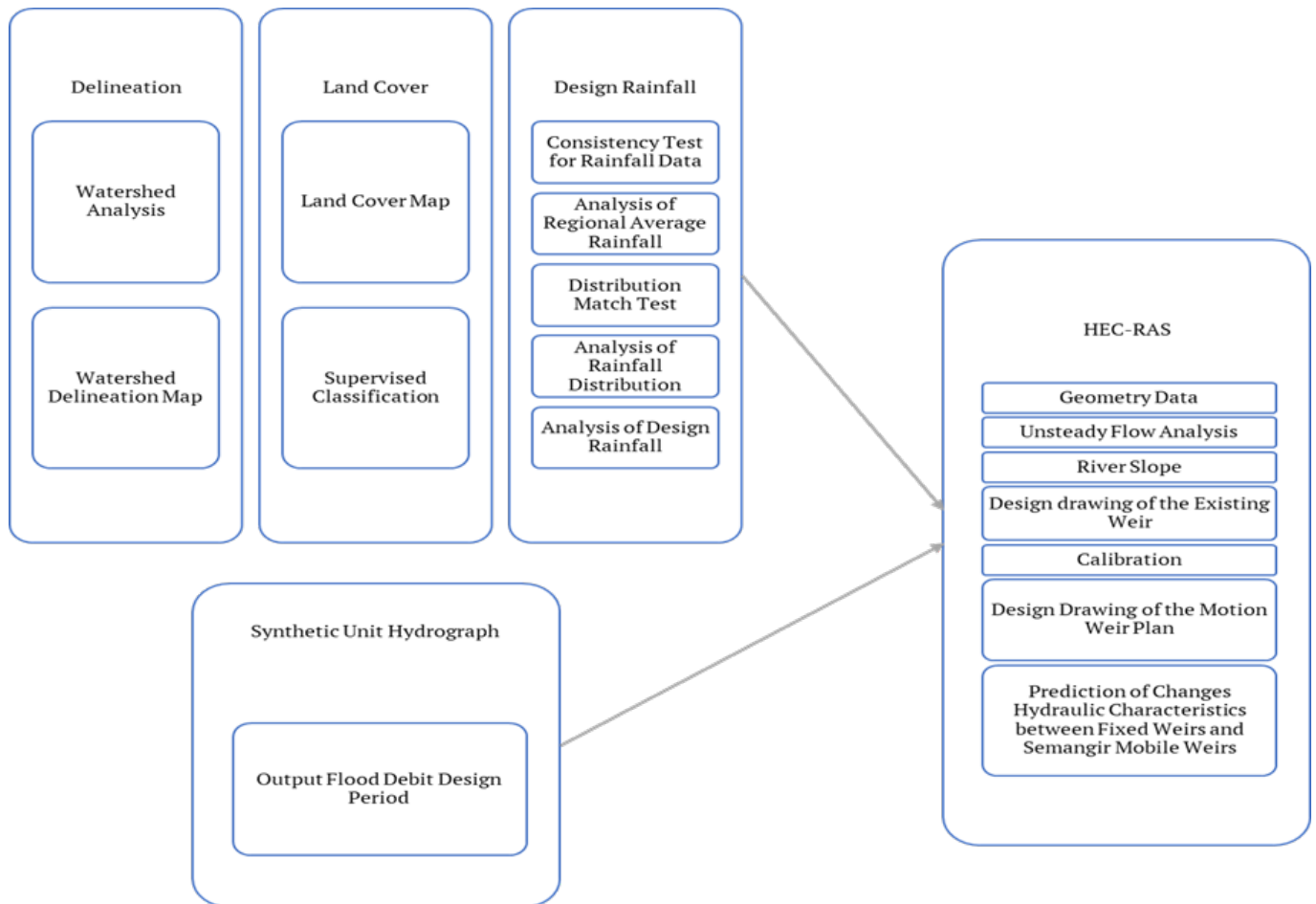


Figure 2 Research stages

2.5 Hydraulic Analysis

The parameters used are Manning's coefficient (roughness value of river cross-sections), geometric data in the form of cross-sections, and river schemes/routes. The flow characteristics of the Semangir River are analyzed with the existing weir and the barrage. Hydraulic characteristics will be analyzed, including flow velocity, water level, and Froude number. Then, the models are compared.

Modeling is done on the fixed weir, then on the design weir, which is a barrage. In this study, two types of barrage gates were used. The first barrage had gates measuring 1.5×1.5 meters, and the second barrage had gates measuring 1.5×0.75 meters. In the modeling of the barrage, two scenarios are used according to the irrigation module with the boundary condition that all water is discharged through the weir gate. The first scenario at the 25-year return period discharge uses the quiet pool operation with a wedge-shaped gate opening, where the gate near the flushing gate is opened higher, then gradually decreases further away from the flushing gate. The second scenario at the 50-year return period discharge opens all gates evenly while the intake gate is closed. If the boundary conditions are not

met, modifications to the weir design will be tried by changing the gate dimensions until the boundary conditions are met.

2.6 HEC-RAS

HEC-RAS is an application program to model river flow River Analysis System (RAS), created by the Hydrologic Engineering Center (HEC), a division within the Institute for Water Resources (IWR) under the US Army Corps of Engineers (USACE). HEC-RAS has four one-dimensional model components: steady flow water surface profile calculations, unsteady flow simulations, sediment transport calculations, and water quality calculations (Bush et al., 2022).

Unsteady flow is a condition where flow velocity, depth, and discharge change over time, with these three parameters being functions of time in unsteady flow cases. The 2D model can provide simulation flow results, while the 1D model only displays tables and graphs (Prawira et al., 2024). Although limited, the 1D model has already provided sufficient results in hydraulic analysis for weir evaluation and simulation.

Hydraulic analysis in channels or rivers is a physical process that follows the laws of mass conservation and momentum conservation (Halik, 2018). The continuity equation can be explained based on the control volume concept described in the mathematical equation of St. Venant. The equation consists of the principles of mass conservation and momentum conservation in the form of partial differential equations, as in Equations (2) and (3).

$$\frac{\partial Q}{\partial x} + \frac{\partial A}{\partial t} - q_{lateral} = 0 \quad (2)$$

$$\frac{\partial Q}{\partial t} + \frac{\partial QV}{\partial x} + gA\left(\frac{\partial z}{\partial x}\right) + S_f = 0 \quad (3)$$

where Q is the flow discharge ($\text{m}^3 \text{s}^{-1}$); t is time (s); A is the total cross-sectional area of the flow (m^2); $q_{lateral}$ is the lateral discharge from the left and right sides of the river ($\text{m}^3/\text{s}/\text{m}$); z is the water surface elevation (m); g is the gravitational acceleration (m s^{-2}); x is the distance measured in the direction of the flow (m); V is the flow velocity (m s^{-1}); and S_f is the energy slope calculated using equation (4).

$$S_f = \frac{n^2|Q|Q}{A^2R^2} \quad (4)$$

2.7 Data Testing and Model-Based Research Results

Hydrological model calibration is the determination of optimal model parameters through parameter settings that match the modeled system. The suitability between model outputs and field observations is compared for model reliability analysis (Shah and Lone, 2022). Verification is an examination or checking of results or data that have been analyzed or collected to obtain accurate results according to actual conditions.

Model performance evaluation involves two approaches: discharge verification of hydrological calculation results, calibration, and validation of the HEC-RAS model against observational data. Model reliability is analyzed with the Root Mean Square Error (RMSE). A higher RMSE value indicates worse model performance, while a lower value indicates better performance and vice versa (Hou et al., 2021). This study uses the RMSE reliability test with equation (5).

$$RMSE = \sqrt{\frac{1}{n} \sum_{i=1}^n (S - O)^2} \quad (5)$$

where S is the simulation result, O is the observation data, and n is the amount of data.

2.8 Barrage

A barrage (vertical) is a weir consisting of a weir body with a low fixed threshold equipped with gates that can be moved vertically or radially. It functions to regulate the water level upstream of the weir and raise the river water level (Irrigation Planning Standard KP-02: Main Structure, 2013).

The gate near the flushing gate is opened higher, then gradually decreases further away from the flushing gate. The gate opening must be such that no water overflows over the top of the gate/weir except for the designed spillway. During large floods with return periods of 50 and 100 years, all gates (barrage, flushing gate, and river flushing gate) are fully opened, while the intake gate is closed.

3 RESULTS

3.1 Hydrological Analysis

Determining the Watershed is done by first determining the weir location as the downstream. After determining the weir location, the watershed boundary is determined with a high contour line as the reviewed boundary. The analysis results obtained a watershed area of 17.31 km^2 and a main river length of 13.13 km , as shown in Figure 1.

Land cover classification in the Semangir sub-watershed is divided into four (4) classes: plantation, settlement, rice field, and dryland/farmland. Based on land cover classification results, the area of each class is as follows: plantation area of 6.58 km^2 , settlement area of 1.74 km^2 , rice field area of 5.55 km^2 , and dryland/farmland area of 3.44 km^2 . Plantation and rice fields dominate the Semangir sub-watershed. The land cover classification results are shown in Figure 3. Based on the land cover, the composite runoff coefficient obtained is 0.28.

In this study, rainfall analysis uses data from four rainfall stations: Dam Manggis, Dam Pono, Dam Sembah, and Dam Semangir. The selection of these rainfall stations is based on the nearest station affecting the Semangir watershed with the downstream at Semangir Weir. The Thiessen polygon method is used to determine the percentage influence of regional rainfall from these four stations. The Thiessen coefficient obtained is 0.1708 at Dam Manggis, 0.1870 at Dam Semangir, 0.0004 at Dam Sembah, and 0.6419 at Dam Pono. The results of the Thiessen polygon calculation are multiplied by consistent rainfall data to obtain regional rainfall data.

Subsequently, frequency distribution analysis will be conducted; however, prior to this, testing will be performed to identify the most suitable distribution for the

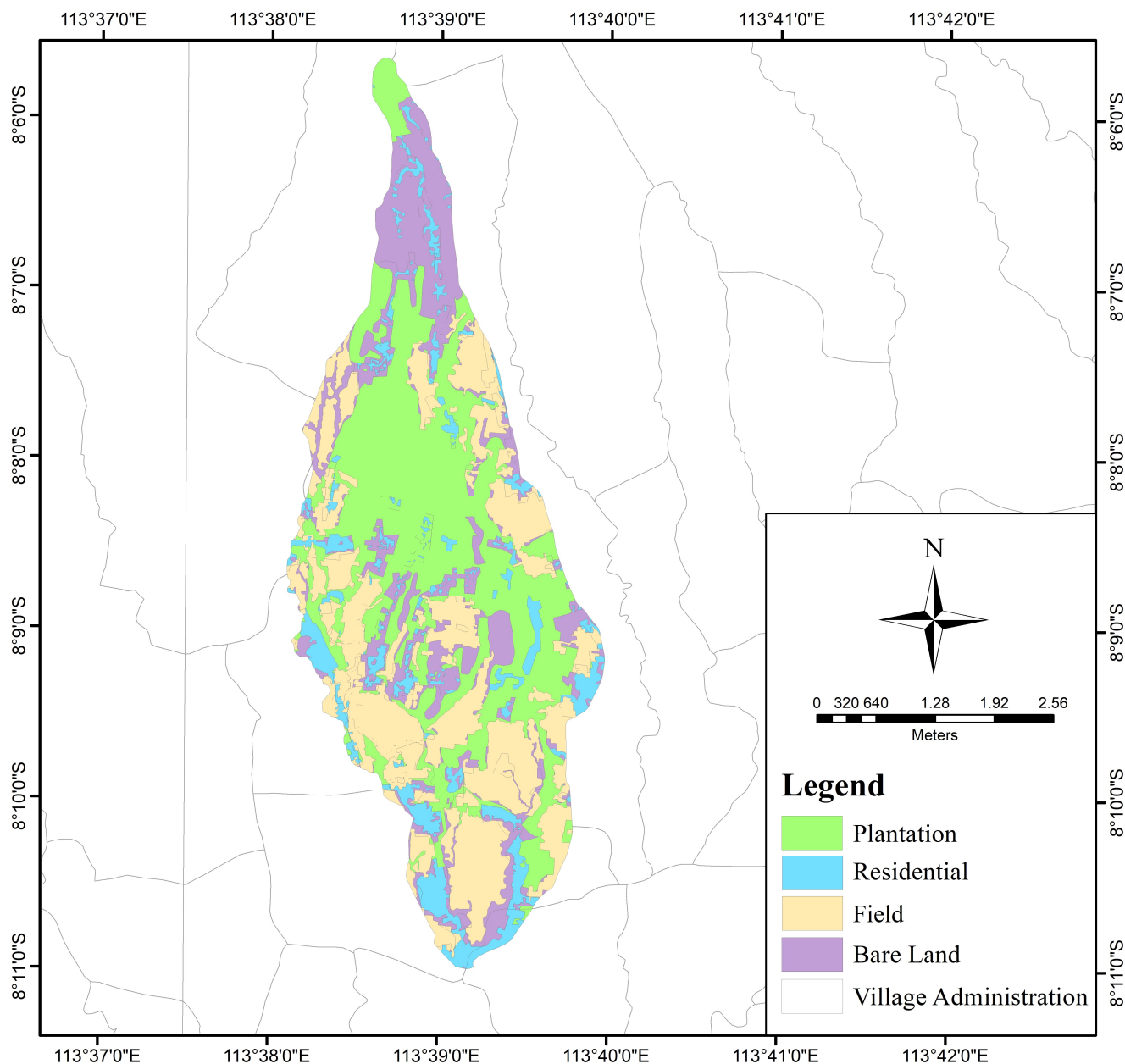


Figure 3 Semangir Sub Watershed land cover map

data. This test involves assessing the regional rainfall data using the Chi-Square and Smirnov-Kolmogorov tests. The Chi-Square test shows that the best distribution is Log-Pearson III and Log Normal, while the Smirnov-Kolmogorov test shows the best distribution is Log-Pearson III. Frequency analysis uses the Log-Pearson III distribution.

The design rainfall obtained is 91.306 mm for the 2-year return period, 120.666 mm for the 5-year return period, 149.264 mm for the 10-year return period, 198.710 mm for the 25-year return period, 247.789 mm for the 50-year return period, and 310.169 mm for the 100-year return period. The research results by Sumanda (2022) in 2022 using the Log Pearson III method obtained design

rainfall for the 2, 5, and 10-year return periods of 106.49 mm, 124.67 mm, and 136.21 mm, respectively. There are several differences in this study; among them, the rainfall data used is 10-year rainfall data from 2011 to 2020 from three rainfall stations: Sta Makam, Sta Pono, and Sta Semangir.

Hourly rainfall intensity analysis was conducted using twelve years of data with the Mononobe method because no hourly rainfall data is available at the rainfall stations. Hourly rainfall distribution is arranged with the Alternating Block Method (ABM) by considering the runoff coefficient. The Alternating Block Method (ABM) is a simple way to create a design hyetograph from the Intensity-Duration-Frequency (IDF)

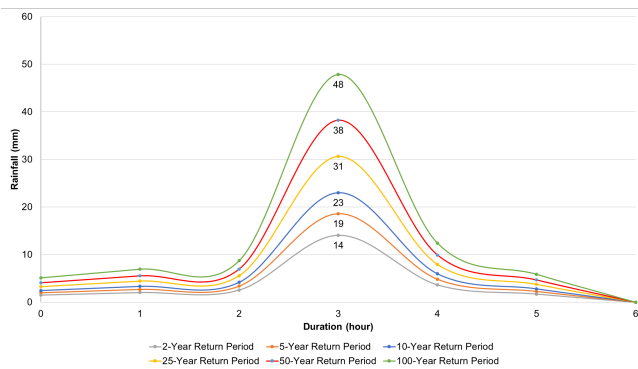


Figure 4 Distribution of Rainfall

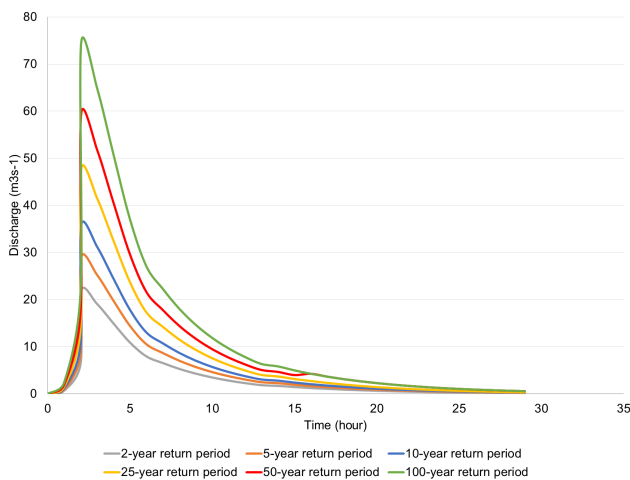


Figure 5 Design Discharge

curve (Chow et al., 1988). For example, the 2-year return period hourly rainfall analysis produces rainfall intensity as follows: Rainfall over 6 hours produces an intensity of 1.51 mm in the 1st hour, 2.05 mm in the 2nd hour, 2.57 mm in the 3rd hour, 14.08 mm in the 4th hour, 3.66 mm in the 5th hour, and 1.73 mm in the 6th hour. The results are shown in Figure 4 according to each return period analysis.

Design flood discharge calculations are used to determine the design discharge that will be used according to SNI 2415:2016. The method chosen for design discharge calculations, based on data availability and watershed characteristics, is the Synthetic Unit Hydrograph (SUH). The SUH used in this research is the SUH Nakayasu.

Design flood discharge calculations using the SUH Nakayasu method produced peak discharges as follows: 21.91 m³ s⁻¹ for the 2-year return period; 28.96 m³ s⁻¹ for the 5-year return period; 35.82 m³ s⁻¹ for the 10-year return period; 47.69 m³ s⁻¹ for the 25-year return period; 59.47 m³ s⁻¹ for the 50-year return period; and 74.44 m³ s⁻¹ for the 100-year return period. The calculations show that the peak flood discharge occurred in the 3rd hour, as shown in Figure 5.

The design flood discharge results were compared with the discharge generated from the water level observation at Semangir Weir. A verification discharge of 53.99 m³ s⁻¹ was obtained, which is between the peak discharges of the 25-year and 50-year return periods. The calculated flood discharge correlated with the observed flood discharge indicates that the calculated discharge is still acceptable and can be used as input data in the modeling. The flood prediction for Yeh Sah River, Bali, Indonesia, using the SCS-CN3 α method with a watershed area of 19.05 km² resulted in the highest peak discharge of 64.17 m³ s⁻¹ (Zahroni et al., 2024). This outcome closely aligns with predictions for this study area despite employing a different method.

3.2 Flood Evaluation in Semangir River

Evaluation is carried out by modeling in the HEC-RAS software. Simulations were conducted on the river with the existing fixed weir to obtain information on water levels and cross-section points that cannot withstand water at return period discharges of 25, 50, and 100 years, as shown in Figure 6. Modeling used flood hydrograph data from previous calculations as the boundary condition at the upstream (Sta 3+800) and downstream (Sta 0+00) using normal depth, which is 0.002.

A further review of flow characteristics at maximum water levels is shown in Table 2. For example, at the 25-year return period, the flow velocity just before the crest is 0.09 m s⁻¹, while the flow velocity after the crest is 1.01 m s⁻¹. The increase in flow velocity is directly proportional to the Froude number.

3.3 Calibration

Calibration was done by comparing the modeled water level at the 50-year return period discharge with field observations. The 50-year return period was chosen because the observed flood discharge verification is between the 25-year and 50-year return periods. The modeling results show the maximum water level at the weir for the return period discharges of 25, 50, and 100 years, respectively, as 1.12 m, 1.26 m, and 1.43 m above the weir crest. The water level data used is the highest observed water level at the Rambipuji Observer UPT PSDA from January to February 2022, which is 1.25 m, as no records were taken during the flood event. The model reliability calculation using RMSE obtained a result of 0.01, indicating good model performance as the RMSE value approaches 0.

3.4 Semangir River's Barrage Modeling

This simulation models the barrage on the Semangir River, replacing the existing fixed weir. The barrage is

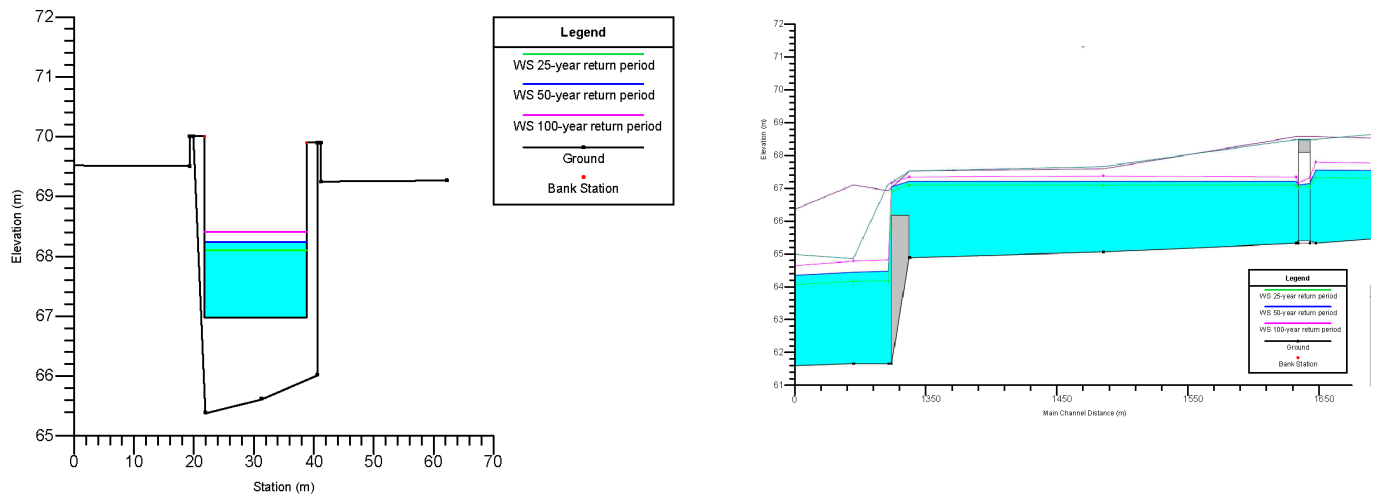


Figure 6 Water Surface Profile of Existing Semangir Weir at 25, 50, and 100-year Return Periods (a) cross-section, (b) long-section

Table 2. Flow Characteristics of the Semangir River

Return period	Discharge	Water Surface Elevation				Velocity		Froude Number	
		Upstream	Downstream	Upstream of Weir	Downstream of Weir	Upstream of Weir	Down-stream of Weir	Upstream of Weir	Downstream of Weir
Years	m ³ s ⁻¹	m	m	m	m	m s ⁻¹	m s ⁻¹		
Q25	47.69	74.45	58.62	67.17	61.96	0.09	1.72	0.02	1.01
Q50	59.47	74.46	58.41	67.17	61.97	0.09	1.68	0.02	0.98
Q100	74.44	74.52	58.68	67.21	62.09	0.11	1.5	0.03	0.8

situated at the same location as the fixed weir, at station 1+431.64, according to the design provided by the UPT PSDA of Jember Regency. The design for the Semangir Barrage- includes nine gates, each measuring 1.5 m × 1.5 m, as illustrated in Figure 7.

Based on HEC-RAS modelling, in Figure 7a, for the 25-year return period at the barrage, the flow profile indicates a velocity of 2.87 m s⁻¹, a water level at an elevation of 68.25 m, and an energy level at an unspecified elevation. The Froude numbers before and after the bridge are 0,73 and 1, respectively. At the weir, the flow profile generally shows a water level at an elevation of 67.75 m, an energy grade elevation of 67.80 m, and an overflowing discharge of 45.26 m³ s⁻¹.

In Figure 7b, the 50-year return period at the bridge, the flow shows the velocity at a speed of 2.87 m s⁻¹, the water level at an elevation of 68.25 m, the energy level at an elevation of m, and the Froude number before and after the bridge are 0.73 and 1. At the weir, the flow profile generally has a water level at an elevation of 67.84 m, an energy level of 67.90 m, and an overflowing discharge of 53.74 m³ s⁻¹.

Because the maximum water level still overflows by 0.06 m above the weir gate, the boundary condition is not met, so re-modeling is done by changing the barrage gate dimensions, subsequently called the modified barrage. A gate with a maximum height of up to 3 m and a width of no more than 3 m is used (Irriga-

tion Planning Standard KP-02: Main Structure, 2013). Remodeling was done with a gate height of 1.75 m and width of 1.5 m, totaling nine gates, as shown in Figure 8. The cross-sections illustrate the Semangir Barrage with 1.5 m × 1.75 m gates during 25- and 50-year flood events. In both scenarios, the water surface upstream is significantly higher than downstream, indicating controlled flow through the barrage. The energy gridline is positioned above the water surface, reflecting the total energy, including kinetic and potential energy. During the 50-year flood, both the energy gridline and water surface are elevated compared to the 25-year flood, highlighting the increased water volume and energy that the barrage manages.

3.5 Comparison of fixed Weir and Design Flow Profiles

Based on Figure 9 and Table 3, the comparison of hydraulic characteristics at the Semangkir Weir reveals significant differences between the fixed weir and the barrage with varying gate dimensions (1.5 × 1.5 m and 1.75 × 1.75 m). Based on simulation results, the fixed weir demonstrates higher energy grade elevation and water surface elevation compared to the barrage. For instance, during the 50-year return period, the energy grade elevation for the fixed weir reaches 2.93 m, while the barrage with a 1.75 × 1.75 m gate only reaches 2.32 m. This indicates that the fixed weir has a greater capacity for energy storage. The findings from the hydraulic analysis are consistent with contemporary

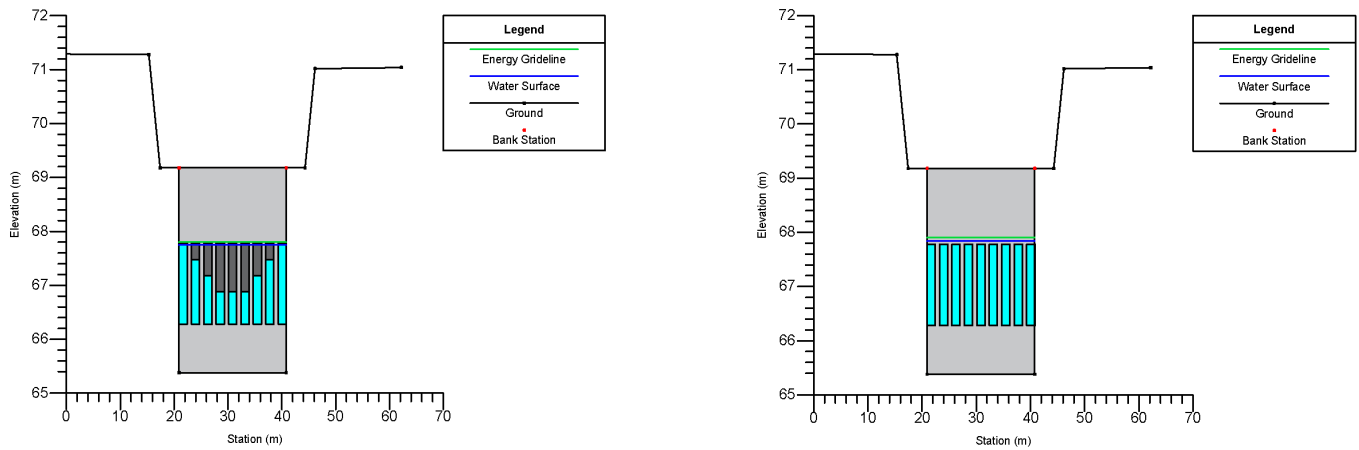


Figure 7 Cross-Section of Semangir Barrage-1 with 1.5 m × 1.5 m Gate during (a) 25 and (b) 50-Year Flood

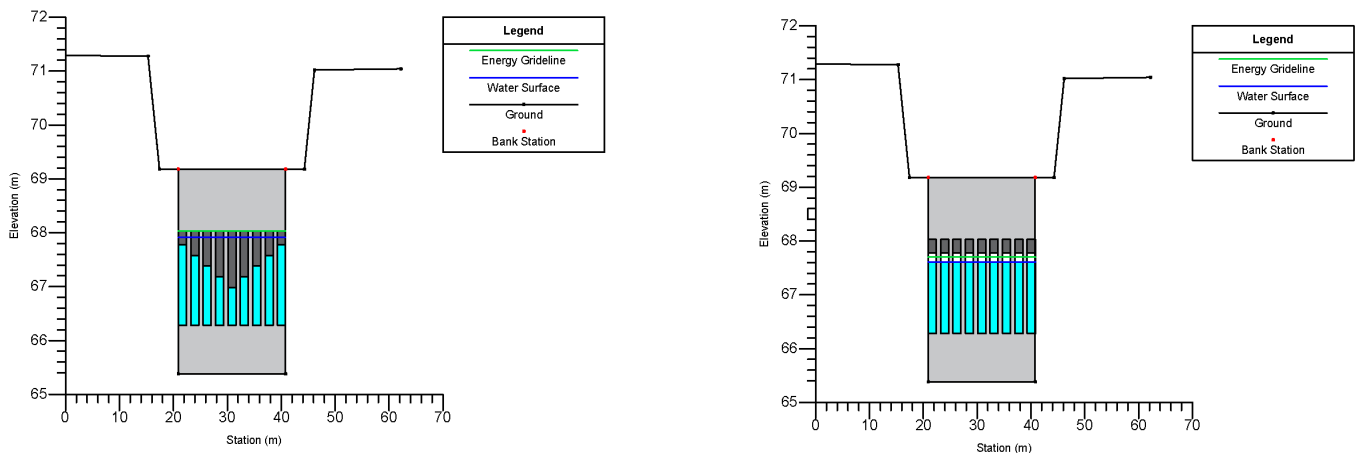


Figure 8 Cross-Section of Semangir Motion Weir with 1.5 m × 1.75 m Gate during 25 and 50-Year Flood

studies on the performance and design of weirs and barrages, reinforcing their distinct functions and hydraulic behavior. The higher energy grade elevation and water surface elevation associated with the fixed weir reflect its suitability for applications requiring consistent energy storage, such as irrigation and hydropower generation. These results are aligned with the seminal work of (Samir et al., 2019), which highlighted the ability of fixed weirs to store and maintain higher energy levels due to their static design that restricts controlled energy dissipation. The fixed weir tends to retain more kinetic energy, which increases pressure on the riverbed and downstream structures, potentially leading to damage (Chanson and Apelt, 2023; Kim et al., 2022).

In Figure 9b, similarly, the greater increase in water surface elevation for the fixed weir (5.15%) compared to the barrage with gates (3.80% and 3.24%, respectively) indicates that the fixed weir is more susceptible to overflow risk during a 50-year flood return period. The barrage demonstrates a better adaptive capa-

bility to control water elevation, making it more effective in flood management (Dickel and Theobald, 2024; Mahlil and Sudinda, 2022). In Table 3, Flow velocity exhibits a different pattern. The fixed weir produces significantly higher downstream velocities, reaching up to 1.72 m s^{-1} during the 25-year return period, compared to the barrage, which only achieves a maximum downstream velocity of 0.94 m s^{-1} . The lower downstream velocity of the barrage highlights its ability to control and dissipate water flow effectively. Additionally, the Froude number downstream of the fixed weir is higher (1.01 during the 25-year return period), indicating a more turbulent and energetic flow compared to the barrage, which exhibits lower Froude numbers (0.83 for the $1.5 \times 1.5 \text{ m}$ gate and 0.64 for the $1.75 \times 1.75 \text{ m}$ gate). This demonstrates that the barrage is more effective in reducing turbulence and mitigating hydraulic impacts downstream. Overall, the fixed weir excels in maintaining higher water surface elevations and energy levels, while the barrage is more suitable for flow control and mitigating hydraulic impacts downstream, particularly with larger gate dimensions.

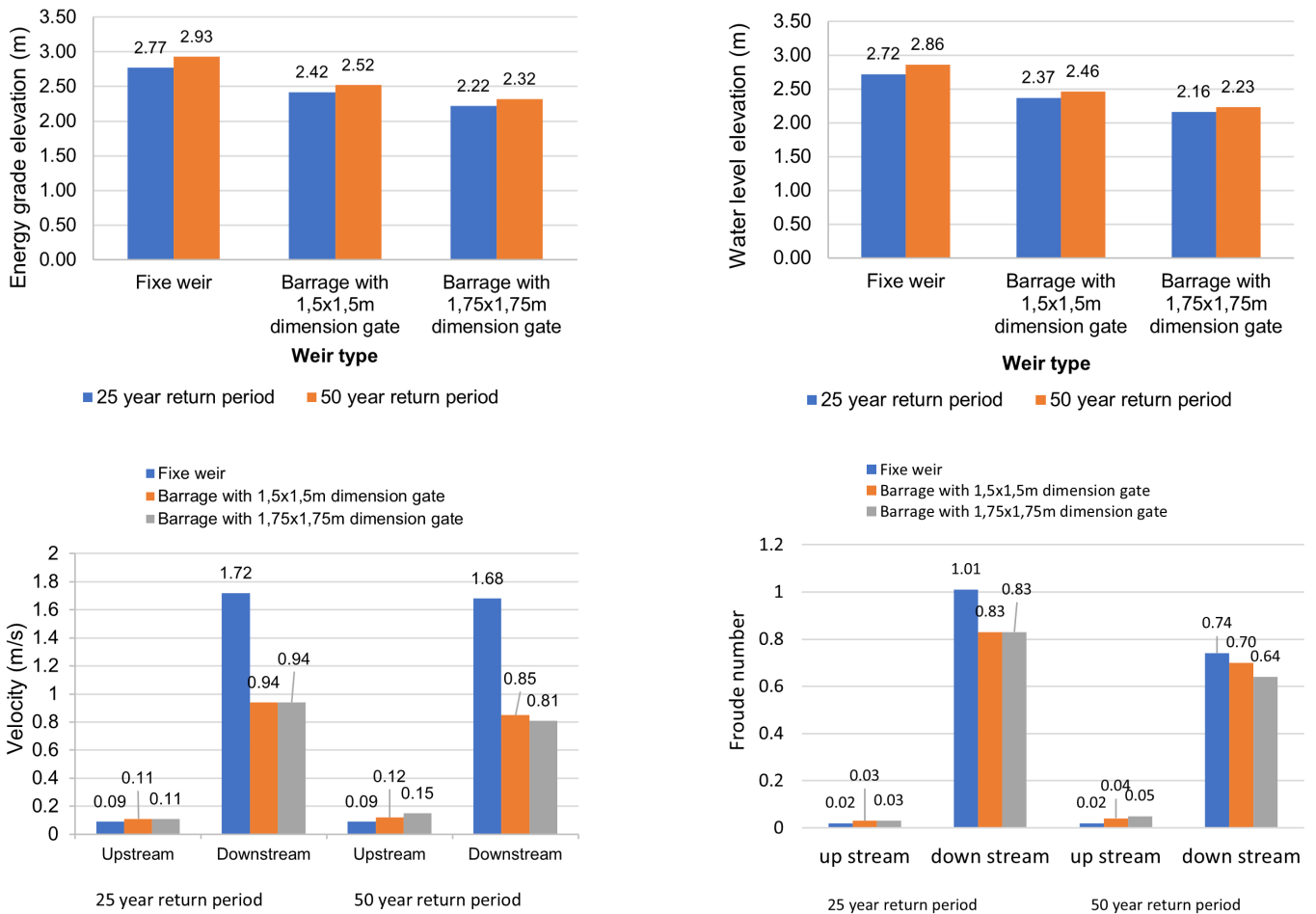


Figure 9 Comparison of the hydraulic behavior of fixed weir and barrage: (a) Energy grade elevation, (b) Water level elevation, (c) Velocity, and (d) Froude number

Table 3. The hydraulic characteristics of the fixed weir and barrage types

Weir/Barrage Type	Return Period (Years)	Energy Grade Elevation (m)	Water Level Elevation (m)	Velocity (m/s) (Upstream/Downstream)	Froude Number (Upstream/Downstream)
Fixed Weir	25	2.77	2.72	0.11 / 1.72	0.03 / 1.01
Fixed Weir	50	2.93	2.86	0.11 / 1.68	0.03 / 0.83
Barrage (1.5 × 1.5 m gate)	25	2.42	2.37	0.09 / 0.94	0.02 / 0.83
Barrage (1.5 × 1.5 m gate)	50	2.52	2.46	0.09 / 0.85	0.02 / 0.70
Barrage (1.75 × 1.75 m gate)	25	2.22	2.16	0.09 / 0.94	0.03 / 0.83
Barrage (1.75 × 1.75 m gate)	50	2.32	2.23	0.15 / 0.81	0.04 / 0.64

However, the fixed weir’s high downstream velocity (1.72 m s^{-1}) and Froude number (1.01 during the 25-year return period) indicate its limitation in controlling flow turbulence downstream, a challenge also highlighted by (Thornton et al., 2014). Their research emphasized that fixed weirs, while effective for water retention, often lead to increased turbulence and erosion potential downstream, impacting both infrastructure stability and aquatic ecosystems.

On the other hand, the barrage demonstrates superior performance in controlling flow and mitigating hy-

draulic impacts downstream, as indicated by its lower downstream velocities and Froude numbers. This aligns with the findings of Kang et al. (2020), who emphasized the flexibility of gated barrages in adapting to dynamic flow conditions and reducing downstream erosion risks. The study highlighted the role of larger gate dimensions, such as the $1.75 \times 1.75 \text{ m}$ gate used in the Semangkir barrage, in enhancing flow control and minimizing hydraulic energy downstream.

The lower Froude number observed for the barrage (0.64 for the $1.75 \times 1.75 \text{ m}$ gate) identifies barrages as

effective structures for reducing turbulence and preserving ecological stability in downstream river systems. This makes barrages particularly suitable for areas where downstream environmental impacts need to be minimized.

Moreover, the adaptability of barrages to extreme hydrological events, such as those induced by climate change, is highlighted in the findings of Kondolf et al. (2014). The study stressed the importance of dynamic flow regulation offered by barrages, enabling them to address flood risks while maintaining downstream ecological balance.

In summary, the results of this study are consistent with previous research, underscoring the fixed weir's ability to maximize energy retention and water storage while the barrage excels in flow regulation and reducing downstream hydraulic impacts. These findings emphasize the importance of selecting the appropriate structure based on specific site conditions and operational objectives, with barrages offering a more flexible and environmentally sustainable solution in areas with fluctuating hydrological conditions or sensitive downstream ecosystems.

4 CONCLUSION

This study confirms that the existing fixed weir at the Semangir River is insufficient for managing the peak discharges of the 25-year and 50-year return periods, which are crucial for effective flood control. By utilizing the HEC-RAS program and conducting simulations with the SUH Nakayasu method, it was determined that the peak discharges are $47.689 \text{ m}^3 \text{ s}^{-1}$, $59.468 \text{ m}^3 \text{ s}^{-1}$, and $74.439 \text{ m}^3 \text{ s}^{-1}$ for the 25-year, 50-year, and 100-year return periods, respectively. The analysis indicates that barrage 2, with gate dimensions of $1.5 \text{ m} \times 1.75 \text{ m}$, provides better than hydraulic performance, significantly lowering the water surface elevation and flow velocity downstream. Specifically, at the 25-year return period, the barrage reduced water surface elevation by 23.63% and flow velocity after the weir by 45%. During the 50-year return period, reductions were 25.61% for water surface elevation and 52% for flow velocity compared to the existing weir. The volume of water released is as follows: fixed weir— $46.46 \text{ m}^3 \text{ s}^{-1}$ for the 25-year return period and $57.57 \text{ m}^3 \text{ s}^{-1}$ for the 50-year return period; Barrage 1— $45.26 \text{ m}^3 \text{ s}^{-1}$ for the 25-year return period and $53.81 \text{ m}^3 \text{ s}^{-1}$ for the 50-year return period; Barrage 2— $46.54 \text{ m}^3 \text{ s}^{-1}$ for the 25-year return period and $57.8 \text{ m}^3 \text{ s}^{-1}$ for the 50-year return period. These results demonstrate that barrages are a viable solution for flood control and water management in the Semangir River, offering enhanced protection against high flow conditions during extreme weather events. This study highlights the effectiveness of barrages for flood control but has limitations, including reliance on simu-

lations, neglecting sedimentation and ecological impacts, and lack of field validation. Future studies should integrate sediment dynamics, ecological assessments, climate change projections, and real-time monitoring to ensure sustainable and reliable flood management solutions.

DISCLAIMER

The authors declare no conflict of interest.

ACKNOWLEDGMENTS

The authors would like to express our sincere thanks and appreciation to the Department of Civil Engineering, Jember University, for their support throughout this research.

REFERENCES

- Balaian, S. K., Sanders, B. F. and Abdolhosseini Qomi, M. J. (2024), 'How urban form impacts flooding', *Nature Communications* **15**(1), 1–10.
URL: <https://doi.org/10.1038/s41467-024-50347-4>
- BNPB (2022), 'Laporan harian pusdalops bnpb (minggu, 08 januari 2023)'.
- Bush, S. T., Dresback, K. M., Szpilka, C. M. and Kolar, R. L. (2022), 'Use of 1d unsteady hec-ras in a coupled system for compound flood modeling: North carolina case study', *Journal of Marine Science and Engineering* **10**(3).
URL: <https://doi.org/10.3390/jmse10030306>
- Chanson, H. and Apelt, C. J. (2023), 'Environmental fluid mechanics of minimum energy loss weirs: hydrodynamics and self-aeration at chinchilla mel weir during the november–december 2021 flood event', *Environmental Fluid Mechanics* **23**(3), 633–659.
URL: <https://doi.org/10.1007/s10652-023-09926-0>
- Chow, V. T., Maidment, D. R. and Mays, L. W. (1988), *Applied Hydrology*, McGraw-Hill Book Co.
- Dickel, S. and Theobald, S. (2024), 'Innovative control strategy for flood mitigation through a combination of barrage management on impounded rivers and polders', *Natural Hazards*.
URL: <https://doi.org/10.1007/s11069-024-06648-4>
- Eizeldin, M. A., Ali, A. M. and Farag, A. M. I. R. A. S. (2023), 'Investigation of flow characteristics downstream vertical sluice gates of bahr yousef regulator physical model', *Water Science* **37**(1), 225–238.
URL: <https://doi.org/10.1080/23570008.2023.2236385>
- Ghimire, E., Sharma, S. and Lamichhane, N. (2020), 'Evaluation of one-dimensional and two-dimensional

hec-ras models to predict flood travel time and inundation area for the flood warning system', *ISH Journal of Hydraulic Engineering* **28**(1), 110–126.

URL: <https://doi.org/10.1080/09715010.2020.1824621>

Guido, B. I., Popescu, I., Samadi, V. and Bhattacharya, B. (2023), 'An integrated modeling approach to evaluate the impacts of nature-based solutions of flood mitigation across a small watershed in the southeast united states', *Natural Hazards and Earth System Sciences* **23**(7), 2663–2681.

URL: <https://doi.org/10.5194/nhess-23-2663-2023>

Halik, G. (2018), *Pemodelan Hidroteknik*, UPT Percetakan dan Penerbitan Universitas Jember.

Hidayah, E., Halik, G., Indarto, I. and Khaulani, D. W. (2022), 'Flood hazard mapping of the welang river, pasuruan, east java, indonesia', *Journal of Applied Water Engineering and Research* pp. 1–12.

URL: <https://doi.org/10.1080/23249676.2022.2114025>

Hou, Y., Zhang, L., Dong, R. Y., Liang, M. Y., Lu, Y., Sun, X. Q. and Zhao, X. (2021), 'Comparing responses of dairy cows to short-term and long-term heat stress in climate-controlled chambers', *Journal of Dairy Science* **104**(2), 2346–2356.

URL: <https://doi.org/10.3168/jds.2020-18946>

Kang, J. N., Wei, Y. M., Liu, L. C., Han, R., Yu, B. Y. and Wang, J. W. (2020), 'Energy systems for climate change mitigation: A systematic review', *Applied Energy* **263**, 114602.

URL: <https://doi.org/10.1016/j.apenergy.2020.114602>

Kim, B. J., Hwang, J. H. and Kim, B. (2022), 'Flow-3d model development for the analysis of the flow characteristics of downstream hydraulic structures', *Sustainability (Switzerland)* **14**(17).

URL: <https://doi.org/10.3390/su141710493>

Kondolf, G. M., Rubin, Z. K. and Minear, J. T. (2014), 'Dams on the mekong: Cumulative sediment starvation', pp. 5375–5377.

URL: <https://doi.org/10.1002/2013WR014979>

Kustamar, K., Susanawati, L. D., Nainggolan, T. H., Witjaksono, A. and Ajiza, M. (2019), 'Performance analysis of long storage and tidal controlling gate on the flood of kemuning river', *Journal of Physics: Conference Series* **1375**(1).

URL: <https://doi.org/10.1088/1742-6596/1375/1/012008>

Mahlil, M. and Sudinda, T. W. (2022), 'Optimization study of gate operation rule in ciawi dam as flood control function', *Jurnal Teknik Sipil* **18**(1), 118–139.

URL: <https://doi.org/10.28932/jts.v18i1.4517>

Mitsopoulos, G., Panagiotatou, E., Sant, V., Baltas, E., Diakakis, M., Lekkas, E. and Stamou, A. (2022), 'Optimizing the performance of coupled 1d/2d hydrodynamic models for early warning of flash floods', *Water*

(Switzerland) **14**(15).

URL: <https://doi.org/10.3390/w14152356>

Nash, J. E. (1957), The form of the instantaneous unit hydrograph, in 'International Association of Hydrological Sciences General Assembly', Vol. 3, Toronto, pp. 114–121.

Ogras, S. and Onen, F. (2020), 'Flood analysis with hec-ras: A case study of tigris river', *Advances in Civil Engineering* **2020**.

URL: <https://doi.org/10.1155/2020/6131982>

Paksi, R. S. J., Dermawan, V. and Andawayanti, U. (2021), 'Kajian hidrolika bangunan pelimpah samping (side channel spillway) bendungan pomalaa kabupaten kolaka provinsi sulawesi tenggara dengan uji model fisik 1:40', *Jurnal Teknologi Dan Rekayasa Sumber Daya Air* **1**(2), 750–763.

URL: <https://doi.org/10.21776/ub.jtresda.2021.001.02.34>

Prawira, A. B., Hidayah, E. and Wiyono, R. U. A. (2024), 'Mapping the lava flood hazard using the flood discharge approach and 2d hydrodynamic modeling at the rejali river, mount semeru', *Journal of the Civil Engineering Forum* pp. 139–150.

URL: <https://doi.org/10.22146/jcef.8463>

Salmasi, F. and Abraham, J. (2023), 'Hydraulic characteristics of flow over stepped and chute spillways (case study: Zirdan dam)', *Water Supply* **23**(2), 851–866.

URL: <https://doi.org/10.2166/ws.2023.011>

Samir, Y., Moussa, A. M. and El-badry, H. M. (2019), 'Hydrodynamic study of nile river using 1d model'.

Sarchani, S., Seiradakis, K., Coulibaly, P. and Tsanis, I. (2020), 'Flood inundation mapping in an ungauged basin', *Water (Switzerland)* **12**(6), 1–21.

URL: <https://doi.org/10.3390/W12061532>

Sari, P., Legono, D. and Sujono, J. (2018), 'Performance of retarding basin in flood disaster risk mitigation in welang river, east java province, indonesia', *Journal of the Civil Engineering Forum* **4**(2), 109.

URL: <https://doi.org/10.22146/jcef.31938>

Shah, M. and Lone, M. A. (2022), 'Flood modeling and simulation using hec-hms/hec-geohms and gis tools for river sindh-nw himalayas', *KN - Journal of Cartography and Geographic Information* **72**(4), 325–333.

URL: <https://doi.org/10.1007/s42489-022-00116-4>

Snyder, F. F. (1938), 'Synthetic unit-graphs', *Eos, Transactions American Geophysical Union* **19**(1), 447–454.

URL: <https://doi.org/10.1029/TR019i001p00447>

Sumanda, V. A. (2022), 'Perencanaan ulang sistem drainase perumahan bumi mangli permai kecamatan kaliwates kabupaten jember'.

Syaifudin, A. (2022), 'Model aliran 2-d untuk memprediksi gerusan dan sedimentasi di saluran jakabaring sport city (jsc) Palembang', *Journal of Water Resources Engineering* **13**(1), 90–99.

Thornton, P. K., Ericksen, P. J., Herrero, M. and Challinor, A. J. (2014), 'Climate variability and vulnerability to climate change: A review', *Global Change Biology* **20**(11), 3313–3328.

URL: <https://doi.org/10.1111/gcb.12581>

Zaffar, M. W., Hassan, I., Latif, U., Jahan, S. and Ullah, Z.

(2023), 'Numerical investigation of scour downstream of diversion barrage for different stilling basins at flood discharge', *Sustainability (Switzerland)* **15**(14).

URL: <https://doi.org/10.3390/su151411032>

Zahroni, A., Nugroho, E. O., Harlan, D., Soentoro, E. A. and Aprilian, Z. (2024), Estimation of debris flow using curve number analysis for the mount agung volcanic event, bali, indonesia, in 'E3S Web of Conferences', Vol. 476, pp. 1–13.

URL: <https://doi.org/10.1051/e3sconf/202447601015>

[This page is intentionally left blank]